CrystEngComm

Accepted Manuscript

ROYAL SOCIETY OF CHEMISTRY

www.rsc.org/crystengcomm

Tuning of net architectures of Ni(II) and Zn(II) coordination polymers using isomeric organic linkers

*Shuang-De Liu, Bing-Chiuan Kuo, Yen-Wen Liu, Jing-Yi Lee, Kwun Yip Wong and Hon Man Lee**

Department of Chemistry, National Changhua Universityf of Education, Changhua 50058, Taiwan, R.O.C.

* To whom correspondence should be addressed. Tel: +886 4 7232105, ext. 3523. Fax: +886 4 7211190. E-mail: leehm@cc.ncue.edu.tw (H.M. Lee).

Abstract: Solvothermal syntheses involving the hybrid ligands {3-pyridin-3-ylimidazo[1,2-a]pyridine (L1) and 3-pyridin-4-ylimidazo[1,2-a]pyridine (L2)}, aromatic polycarboxylates [1,4-benzenedicarboxylate (1,4-bdc), 1,3-benzenedicarboxylate (1,3-bdc), and 1,3,5-benzenetricarboxylate (1,3,5-btc)], and transition metal ions [Ni(II) and Zn(II) ions] afforded five new coordination polymers, namely, $[Ni(1,4\text{-bdc})(L1)(H_2O)_2]_n$ (**1**), $[Ni_2(1,3\text{-bdc})_2(L1)_2(H_2O)]_n$ (**2**), $[Zn_2(1,4\text{-bdc})_{1.5}(L1)(OH)]_n$ (**3**), and $[Zn_2(1,3,5\text{-btc})(L1)O_{0.5}(H_2O)_{0.5}\cdot 0.5H_2O]_n$ (**4**) and $[Zn_2(1,3,5\text{-btc})(L2)(OCOH)(H_2O)]_n$ (**5**). A diversity of net topologies was observed including a rare 2D 4-connected net with the point symbol of $(4^4.6^3.8)$ in **1**, a **dia** net in **2**, a two-fold interpenetrating **pcu** net in **3**, a rare 3D (3,8)-connected binodal **3,8T35** net in **4**, and **sra** and **rtl** nets in **5**. Four different secondary building units were involved in the construction of the 3D nets. The three Zn(II) complexes exhibit photoluminescence.

Introduction

Coordination polymers (CPs) or metal-organic-frameworks (MOFs) have received much attention because they have potential applications in diverse areas[1] such as luminescence,[2] magnetism,[3] ion exchange,[4] drug delivery,[5] catalysis,[6] gas storage,[7] sensor,[8] and separation.[9] Therefore, the design and syntheses of CPs with desirable architectures and topologies is a subject of intense interest.[10] Previously studies have firmly established that the use of rigid bipyridine ligands[11] and, to a lesser extent, bis-imidazole-based ligands[12] in combination with aromatic polycarboxylates as secondary ligands could afford a wide scope of intriguing multi-dimensional CPs with transition metal ions. In this regard, we have recently reported the utilization of bis-imidazole derivatives as organic linkers to produce a variety of CPs with interesting net topologies.[12f-h] Rather surprisingly, hybrid ligands consisting of pyridine and imidazole subunits have been rarely employed in the constructions of CPs.[13] The inaccessibility of these ligands from commercial available starting materials might be one of the reasons. To continue our effort on obtaining novel CPs with interesting net architectures, we designed two hybrid ligands as new organic linkers (Chart 1). They are an isomeric pair and can be synthesized very easily via a Pd-catalyzed direct C–H arylation of imidazo[1,2-a]pyridine and bromopyridines.[14] Also, desirably, these new organic linkers containing polyaromatic rings exhibit strong emission properties. We envisioned that the utilization of these new organic linkers in combination with a variety of aromatic polycarboxylates including 1,4-benzenedicarboxylate (1,4-bdc), 1,3-benzenedicarboxylate (1,3-bdc), and 1,3,5-benzenetricarboxylate (1,3,5-btc) as secondary ligands could allow a diverse type of multi-dimensional CPs to be produced. Pleasingly, the tuning of net architectures by utilizing these two sets of ligands formed CPs with Ni(II) and Zn(II) ions which exhibit different frameworks including **dia**, **pcu**, **sra**, **rtl** topologies, etc. Also interestingly

in this study, we demonstrated that the heating temperature and duration of the solvothermal conditions were crucial in controlling the phase purity of the crystalline materials. The luminescence properties of the three new Zn(II) CPs were also investigated.

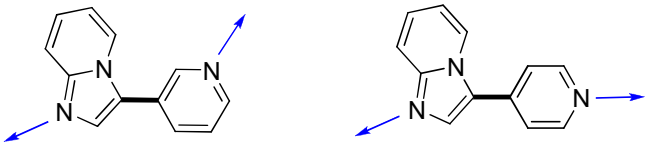

Chart 1. 3-Pyridin-3-ylimidazo[1,2-a]pyridine (L1) and 3-pyridin-4-ylimidazo[1,2-a]pyridine (L2) as organic linkers for the construction of CPs.

Results and discussion

Synthesis and characterization of CPs. Instead of traditional cross-coupling reactions involving multi-step synthesis, recent advances in Pd-catalyzed direct C–H arylation allows the preparation of the hybrid ligand (L1 and L2) from commercial available imidazo[1,2-a]pyridine and bromopyridines in a single step.[14] The new pure complexes $[Ni(1,4\text{-bdc})(L1)(H_2O)_2]_n$ (**1**), $[Ni_2(1,3\text{-bdc})_2(L1)_2(H_2O)]_n$ (**2**), $[Zn_2(1,4\text{-bdc})_{1.5}(L1)(OH)]_n$ (**3**), and $[Zn_2(1,3,5\text{-btc})(L1)O_{0.5}(H_2O)_{0.5}\cdot 0.5H_2O]_n$ (**4**) were prepared by solvothermal syntheses involving the respective hybrid ligands, benzenecarboxylic acids, and metal precursors in a 8:2 water/DMF mixture at 140 ºC for a total duration of 48 h (condition A). $[Zn_2(1,3,5\text{-btc})(L2)(OCOH)(H_2O)]_n$ (**5**) was obtained by a similar procedure but heating at 150 ºC for a total duration of 25 h (condition B). Crystalline products were obtained with yields in the range of 50–95 %. Each compound was characterized by elemental analysis, IR spectroscopy, PXRD studies, and X-ray crystallographic analysis (Table 1–4 and Table S1 in the ESI†). The phase purities of **1**–**5** were confirmed by comparing their PXRD patterns with those simulated from single-crystal X-ray diffraction studies (Fig. S1–5 in the ESI†).

Structural descriptions. Complex **1** crystallizes in the orthorhombic space group F*dd*2. An asymmetric unit of **1** consists of a Ni atom, 1,4-bdc, L1, and two coordinated water molecules. The Ni atom adopts octahedral coordination geometry, coordinated by a pyridyl N and an imidazolyl N from two L1 ligands, two η^1 carboxylate O atoms from two dicarboxylates, and two water molecules (Fig. 1a). The two carboxylic O atoms are trans to each other, whereas the two N atoms as well as the two O atoms adopt cis dispositions. The Ni–N bonds are 2.097(4) and 2.062(4) Å and the Ni–O bonds fall in the range of 2.036(4)–2.113(4) Å. The bond distances between the Ni atom and the O atom of the coordinated water molecules are longer than those of carboxylate O atoms [2.113(4) and 2.092(4) Å vs. 2.044(3) and 2.036(4) Å]. The 1,4-bdc ligands link the Ni atoms into two sets of 1D chains running approximately orthogonal to each other. The L1 ligands connect these chains into an infinite 2D layer along the *ac* plane (Fig. 1b). To understand the topology of the underlying net in **1**, analysis using the TOPOS software was performed.[15] The simplification of the network treating the Ni atoms as nodes and the two types of ligands as linkers revealed a rare 2D 4-connected net (Fig. 1c). The point symbol[16] is $(4^4.6^3.8)$. These 2D layers were further linked by hydrogen bonds between the H atoms of the water molecules and the carboxylate O atoms, resulting in an overall 3D network (Table S2 in the ESI†). Solvent-accessible space exists in the structure which is 412.8 $Å^3$ (5.3 % per unit cell volume) according to PLATON.[17]

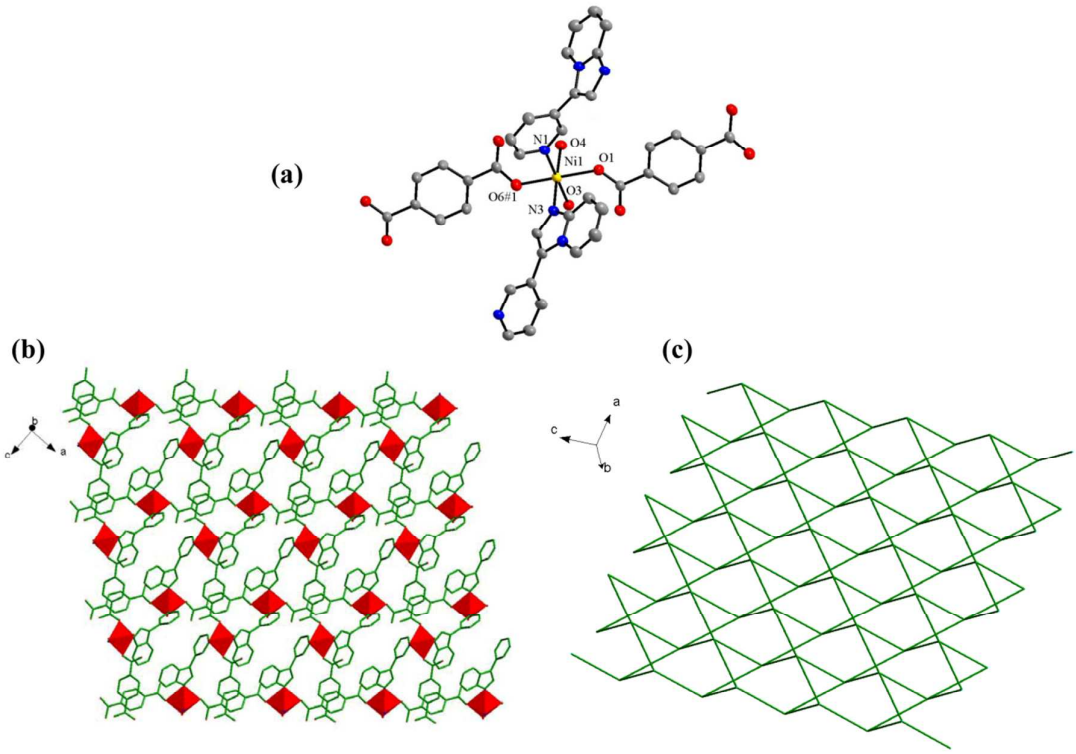

Fig. 1. (a) Coordination environment of the Ni center in **1** with thermal ellipsoids shown at 50 % probability. The hydrogen atoms are omitted for clarity. Symmetry code: #1 = x + 1/2, y, z − 1/2. (b) View of the 2D 4-connected net in **1**. (c) Topological representation of the 2D 4-connected net in **1**.

Instead of terephthalic acid (1,4-bdcH_2), the isomeric isophthalic acid (1,3-bdcH_2) was used in the synthesis of **2**, leading to an intriguing 3D framework. Complex **2** also crystallizes in the orthorhombic space group F*dd*2. An asymmetric unit consists of a Ni atom, 1,3-bdc, L1, and one half of water molecule. The O atom of the coordinated water sits on a crystallographic two-fold axis. The Ni center is in octahedral coordination geometry, defined by three carboxylate O atoms from three 1,3-bdc ligands, cis pyridyl and imidazolyl N atoms from two L1 ligands, and an O atom from the coordinated water that is trans to the pyridine N atom (Fig. 2a). Two of the coordinated carboxylate groups and the coordinated water molecule operate in μ^2-η^1:η^1- and μ^2-bridging modes, respectively, connecting two Ni atoms to form a dinuclear $Ni_2(CO_2)_2(\mu\text{-}H_2O)$ secondary building unit (SBU)[18] (Fig. 3a). The bond distance between Ni and μ-O atoms

is 2.0348(16) Å, whereas the Ni–O distances from the carboxylate O atoms vary in the range of 2.015(2)–2.096(2) Å. The non-bonding distance between two adjacent Ni atoms is ca. 3.5436(7) Å. The L1 and 1,3-bdc ligands act as linkers joining the SBUs into a 3D framework (Fig. 2b). The topology of the 3D net in **2** was analyzed by TOPOS software. Taking the consideration of SBUs as cluster nodes, the underlying net of **2** can be described as a uninodal **dia** topology, which is one of the most frequent nets observed for CPs (Fig. 2c).[19] A large solvent void space of 1769.2 $Å^3$ (21.2 % per unit cell volume) presents in the framework of **2** according to PLATON.

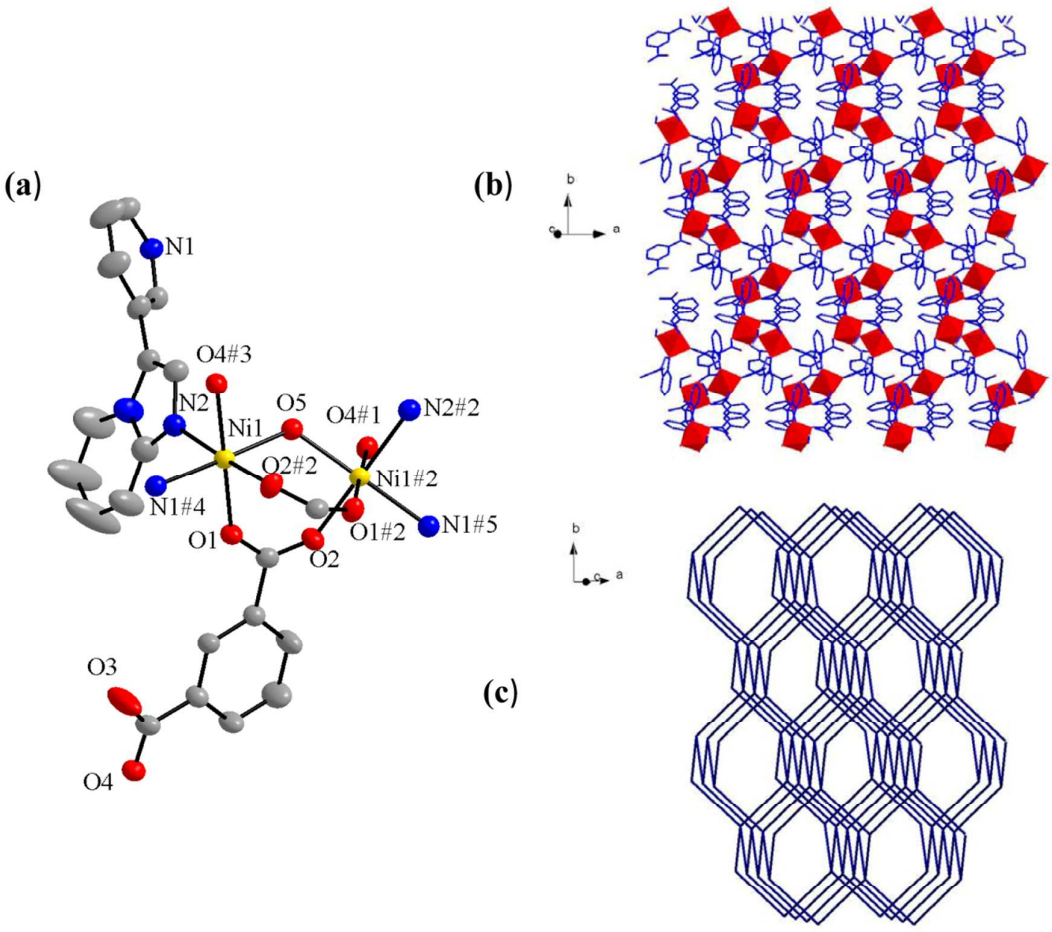

Fig. 2. Coordination environment in **2** with thermal ellipsoids shown at 50 % probability. The hydrogen atoms are omitted for clarity. Symmetry code: #1 = x + 1/4, –y + 1/4, z + 1/4; #2 = –x + 2, –y, z; #3 = –x +

7/4, y – 1/4, z + 1/4; #4 = x – 1/4, –y + 1/4, z – 1/4; #5 = –x + 7/4, y – 1/4, z – 1/4. (b) View of the 3D net in **2** viewing along the [101] direction (c). Topological representation of the 3D **dia** net in **2**.

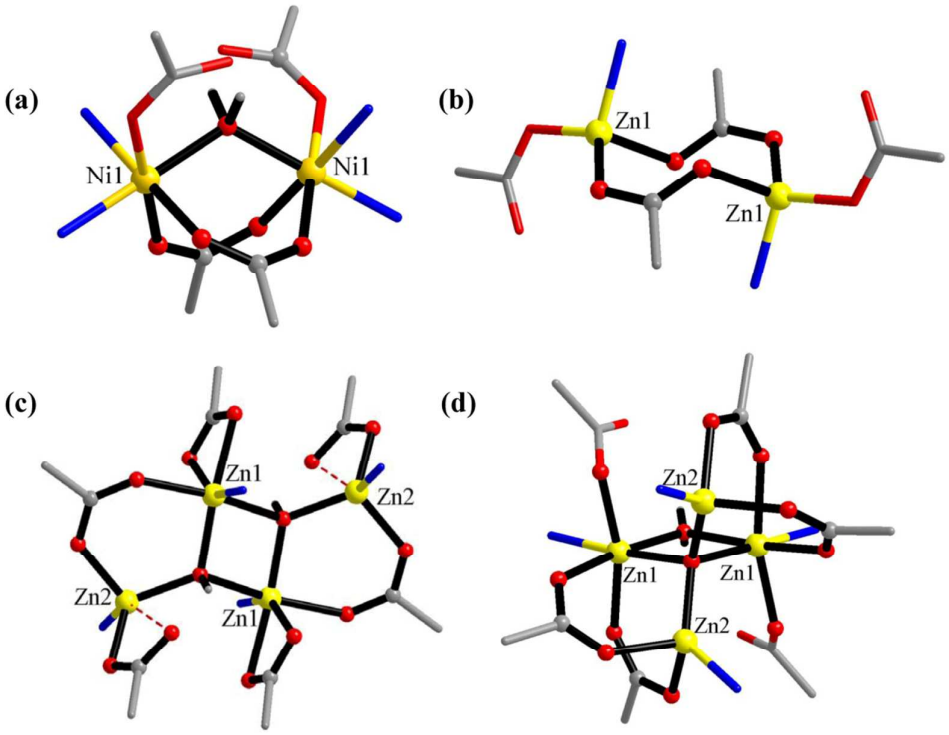

Fig. 3. Ball-and-stick representation of SBUs. (a) Dinuclear $Ni_2(CO_2)_2(\mu\text{-}H_2O)$ cluster unit in **2**. (b) Dinuclear $Zn_2(CO_2)_4$ cluster unit in **5**. (c) Tetranuclear $Zn_4(CO_2)_6(\mu^3\text{-}OH)_2$ cluster unit in **3**. (d) Tetranuclear $Zn_4(CO_2)_4(\mu^4\text{-}O)(\mu\text{-}H_2O)O_2$ cluster unit in **4**.

Beside nickel CPs, we were also interested to prepare zinc CPs for their potential applications as luminescence materials.[2] Thus replacing $Ni(NO_3)_2{\cdot}6H_2O$ with $Zn(NO_3)_2{\cdot}6H_2O$ in the solvothermal synthesis involving L1 and 1,4-bdcH_2 afforded **3**. The change of metal ion from Ni(II) to Zn(II) results in a totally different coordination framework with respect to that in **1**. Complex **3** crystallizes in the triclinic space group $P\bar{1}$. An asymmetric unit consists of two Zn atoms, one and a half molecule of 1,4-bdc, a full molecule each of L1 and a hydroxide ligand. The Zn1 atom is in octahedral coordination environment, consisting of a pyridyl N atom, three carboxylate O atoms from two 1,4-bdc ligands, and two cis OH ligands (Fig. 4a). One

of the 1,4-bdc ligands is in chelating mode, whereas the other one operates in μ^2-η^1:η^1-bridging mode, connecting Zn1 and Zn2 atoms. Interestingly, O7 atom from the hydroxide ligand operates in a μ^3-bridging mode, linking 2Zn1 and Zn2 atoms (Zn–O distances = 2.040(2) and 1.949(2) Å). In contrast, the coordination environment around Zn2 can be described as a distorted tetrahedral, defined by an imidazolyl N atom, two carboxylate O atoms from two 1,4-bdc ligands, and an O atom from the hydroxide ligand. The average bond angle of Zn2 is 109.3 º that is about the ideal bond angle of a tetrahedron. One of the carboxylate O atoms is from a bridging 1,4-bdc ligand. The other O atom coordinates to the Zn2 atom in a monodentate fashion. Notably, the non-bonding O3#5 atom from the same carboxylate group is in close contact with Zn2 with a non-bonding distance of 2.790 Å (see Fig. 3a). Overall, six carboxylate groups and the two μ^3-OH ligands link four Zn centers together forming a $Zn_4(CO_2)_6(\mu^3\text{-}OH)_2$ tetranuclear metal cluster (Fig. 3c). Although ten organic linkers were connected to the cluster unit, four pairs were parallel to each other such that it functions as a six-connected octahedral SBU. These SBUs are joined by ditopic linkers to form a 3D framework (Fig. 4b). The topology of the underlying net was further analyzed by TOPOS, revealing a 3D uninodal net of **pcu** framework (Fig. 4c). CPs of **pcu** topology are commonly observed in the literature.[19] Importantly, two-fold interpenetration of the **pcu** frameworks exists (class **1a**),[20] limiting the void space in the structure. It is worth noting that a SBU of the same $Zn_4(CO_2)_6(\mu^3\text{-}OH)_2$ unit has recently been reported.[21] However, this cluster unit in $[Zn_4(\mu_3\text{-}OH)_2(TPO)_2(H_2O)_2]$ (H_3TPO = tris(4-carboxylphenyl)phosphine oxide)) is eight-connected, instead of six-connected in **3**. The cluster units are further connected by TPO^{3-} ligands to form a 3D 3,8-connected net of **flu** topology.

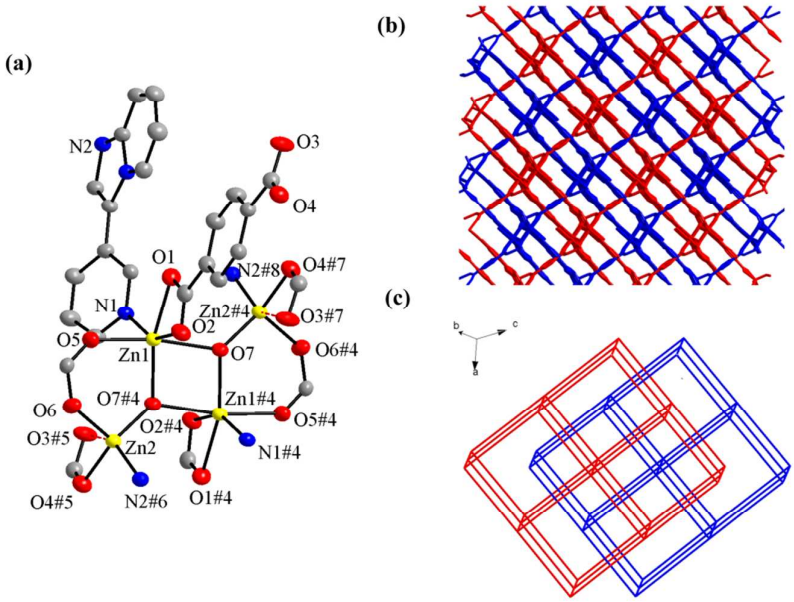

Fig. 4. (a) Coordination environment of the tetranuclear zinc unit in **3** with thermal ellipsoids shown at 50 % probability. The hydrogen atoms are omitted for clarity. Symmetry code: #1 = –x + 2, –y + 2, –z + 1; #2 = x + 1, y, z + 1; #3= x, y + 1, z + 1; #4 = –x + 1, –y + 1, –z; #5 = –x + 2, –y + 1, –z. (b) View of the 3D net in **3** viewing along the [011] direction. (c) Schematic view of the two-fold interpenetrating **pcu** net in **3**.

After we obtained **3** featuring L1 and 1,4-bdc as ligands, attempts were then made to prepare Zn CP employing the isomeric 1,3-bdc as ditopic organic linker. However, such complex was not obtained under the solvothermal conditions. Instead we could employ 1,3,5-benzenetricarboxylic acid (1,3,5-btcH_3) to prepare **4**. Complex **4** crystallizes in the monoclinic space group *C*2/*c*. An asymmetric unit consists of two Zn atoms, 1,3,5-btc, L1, and one half each of a μ^4-oxo and a μ^2-H_2O molecule. The latter two O-donor ligands are situated on a crystallographic two-fold axis. The coordination geometry around the Zn1 atom can be described as a distorted octahedron, defined by a pyridyl N atom, the O atom from the μ-H_2O ligand, the O atom from the μ^4-oxo ligand, and three carboxylate O atoms from three 1,3,5-btc ligands (Fig. 5a). Contrastingly, the Zn2 atom is in tetrahedron coordination geometry featuring an imidazolyl N atom, the O atom of μ^4-oxo ligand, and two carboxylate O atoms from two 1,3,5-btc ligands. Due to the bridging

coordination modes of the four carboxylate groups, the μ^4-oxo, and the μ-H_2O ligands and together with two O atoms from two carboxylate groups, a $Zn_4(CO_2)_4(\mu^4\text{-}O)(\mu\text{-}H_2O)O_2$ tetranuclear cluster was formed (Fig. 3d). Other Zn_4O cluster units were observed in various MOFs.[18, 22] The central O atom is tetrahedrally surrounded by four Zn atoms. The bond distances between the Zn atoms and the oxo ligands are 1.903(3) and 2.052(4) Å. The Zn1 and Zn2 atoms are in close contact within the cluster with a non-bonding distance of 3.015(2) Å. The Zn1···Zn1 and Zn2···Zn2 distances, which are 3.292(1) and 3.359(1) Å, respectively, are significantly longer. Noteworthy, the structure of this SBU is quite different from that of **3** (*vide infra*). In the cluster of **4**, all the four Zn atoms are directly connected to each other via the μ^4-oxo ligand, whereas in that of **3**, three of the four Zn atoms are connected via the μ^3-OH ligand (see Fig. 3c and d). The tetranuclear Zn clusters are interconnected by organic linkers forming a 3D net (Fig. 5b). The topology of **4** was analyzed by TOPOS software,[15] revealing an interesting topology. The C_6H_3 moiety of the 1,3,5-btc ligand can be considered as a three-connected node. The tetranuclear cluster is the SBU functioning as an eight-connected node. Based on this simplification, **4** exhibits a rare 3D (3,8)-connected binodal **3,8T35** topology (Fig. 5c). The point symbol[16] for the 3D net is $(3.4.5)_2(3^4.4^4.5^2.6^6.7^{10}.8^2)$. A total solvent void space of 378.6 $Å^3$ (9.3 % per unit cell volume) exists in the framework of **4** according to PLATON.

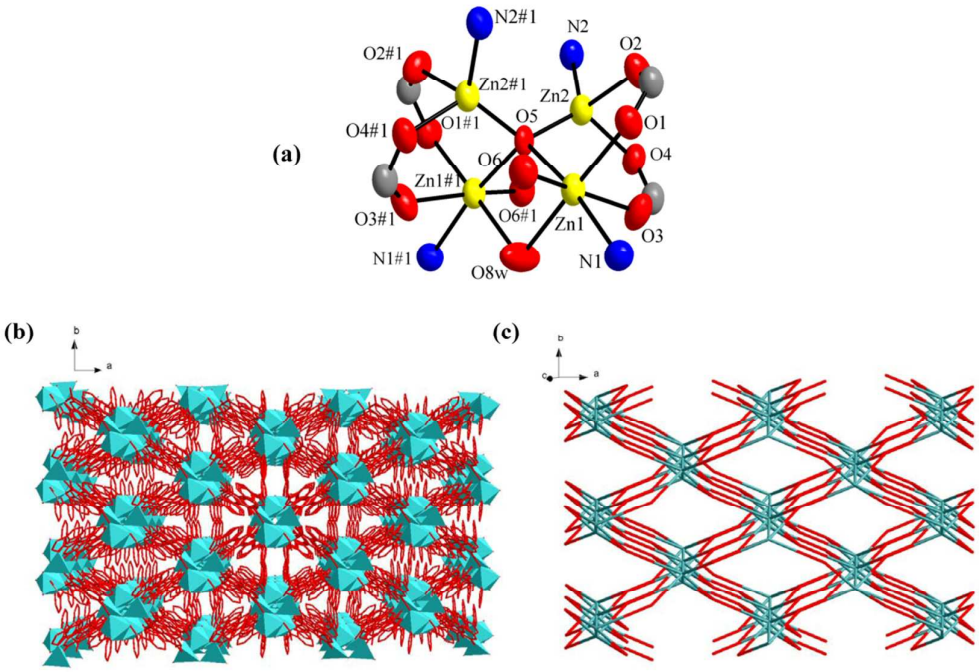

Fig. 5. (a) Coordination environment of the tetranuclear zinc unit in **4** with thermal ellipsoids shown at 50 % probability. The hydrogen atoms are omitted for clarity. Symmetry code: #1 = –x, y, –z + 1/2. (b) View of the 3D net in **4** viewing along the [001] direction. (c) Schematic view of the 3,8-connected net in **4**.

Employing the same heating program for **1**–**4** (condition A), we successfully utilized the isomeric L2 in combination with 1,3,5-btc as ligands to obtain **5**, the structure of which was established by X-ray crystallography. The complex crystallizes in the monoclinic space group $P2_1/c$. An asymmetric unit consists of two Zn atoms, one unit each of 1,3,5-btc, L2 and H_2O ligand, and surprisingly, a format ligand. The formation of the format ligand was presumably due to the decomposition of DMF solvent under the solvothermal condition.[23] The Zn1 atom is in tetrahedral coordination environment, ligated by an imidazolyl N atom and three O atoms from three 1,3,5-btc ligands (Fig. 6a). The average bond angle around Zn1 atom is 109.1 Å. The Zn2 atom is five-coordinated featuring a pyridyl N atom, an O atom from H_2O, two O atoms from a chelating carboxylate group, and the O atom of the format ligand. There is a long contact between Zn2 and O6 with a contact distance of 2.463(4) Å, resulting in the seemingly chelating carboxylate group

coordinated to the metal center. The corresponding O–Zn–O bite angle is 58.08(16) Å. As a result, the coordination geometry around the Zn2 atom can be described as a highly distorted trigonal bipyramid with O6 and O8 occupying the axial positions [∠O6–Zn2–O8 = 165.09(18)º]. The two sets of ligands connect the Zn ions into a 3D network (Fig. 6b). From the topological point of view, Zn1 atoms and 1,3,5-btc ligands can be regarded as 4-connected nodes of the underlying net. The overall topology can then be described as a 3D uninodal net of **sra** topology (Fig. 7a). CPs with **sra** nets are much rarer relative to the above-mentioned **dia** and **pcu** nets and recently several examples have been reported in the literature.[19, 24] Alternatively, the dimeric $Zn_2(CO_2)_4$ consisting of 2Zn1 atoms can be regarded as a six-connected SBU (Fig. 3b), whereas the 1,3,5-btc acts a three-connected node. The topological analysis then showed that **5** exhibits a 3D net with a 3,6-connected binodal **rtl** topology (Fig. 7b). CPs with **rtl** topology are still rare.[19, 25] The framework in **5** is closely packed such that no solvent accessible void is present.

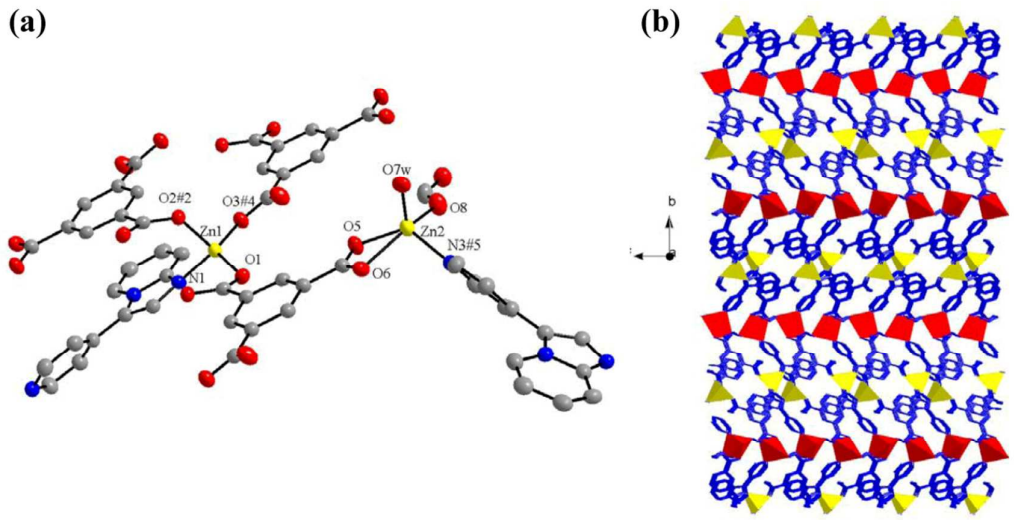

Fig. 6. (a) Coordination environment of the Zn atoms in **5** with thermal ellipsoids shown at 50 % probability. The hydrogen atoms are omitted for clarity. Symmetry code: #1 = –x + 1, y + 1/2, –z + 1/2; #2 = –x + 1, –y + 2, –z + 1; #3 = x – 1, y, z – 1; #4 = x + 1, y, z + 1; #5 = –x + 1, y – 1/2, –z + 1/2. (b) View of the 3D net in **5** viewing along the [100] direction.

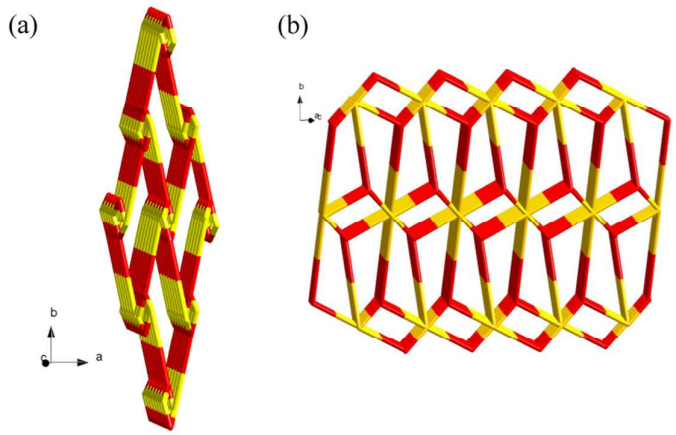

Fig. 7. (a) Schematic view of **sra** net in **5**. The 4-connected nodes are shown in red and yellow. (b) Schematic view of **rtl** net in **5** based on the dimeric SBUs. The 3- and 6-connected nodes are shown in red and yellow respectively.

The phase purity of the sample was then checked and as indicated by the PXRD traces of the as-synthesized sample and the theoretical pattern of **5** another solid phase is present (Fig. 8). Subsequently, a crystal was successfully picked and the structure of $[Zn(1,3,5\text{-btcH})(L2)(H_2O)\cdot(H_2O)]_n$ (**6**) was established by X-ray diffraction study. Compound **6** crystallizes in the triclinic space group $P\bar{1}$. An asymmetric unit contains a Zn atom, a unit each of L2, 1,3,5-btcH, a coordinated H_2O, and a water solvent molecule. The Zn atom is in trigonal bipyramidal coordination geometry, defined by an imidazolyl N atom, an O atom of water ligand, and three O atoms from three 1,3,5-btcH ligands (see Fig. S6 and Table S3 in the ESI†). The O atom of the water ligand and the bridging O atom of one of the 1,3,5-btcH ligands occupy the axial positions. Importantly, one of the carboxylic groups is un-deprotonated and the pyridyl N atom of L2 is uncoordinated. As a result, only the ditopic 1,3,5-btcH ligands link the metal centers into 1D ladder polymeric chains (see Fig. S7 in the ESI†).

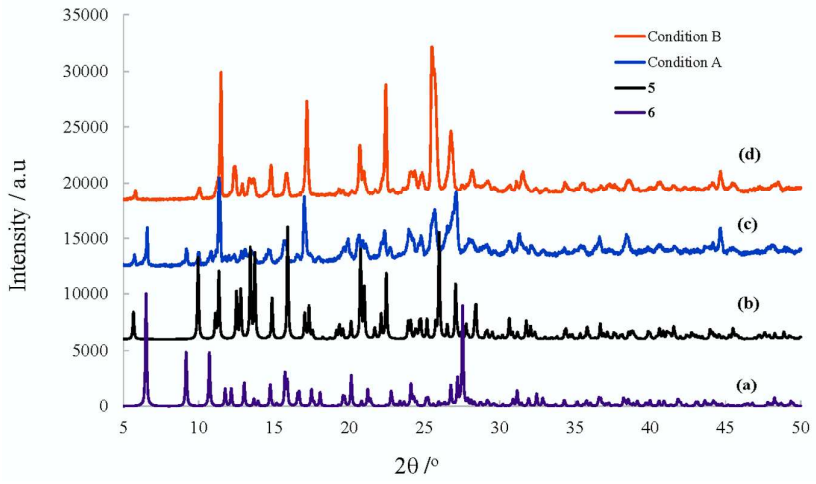

Fig. 8. PXRD patterns: (a) simulated from the single crystal data of **6**, (b) simulated from the single crystal dat of **5**, (b) as-synthesized from condition A, and (d) as-synthesized from condition B.

Attempts were then made to obtain a pure phase by varying the reaction parameters such as the heating temperature, ratio of solvent mixture, and molar ratio of metal to ligand precursor. Pleasingly, by varying the heating program (condition B: 150 ºC for 25 h instead of 140 ºC for 48 h), pure **5** was obtained as indicated by the PXRD traces (see Fig. 8). In fact, in the case of 1–4, preliminary studies showed that by varying the reaction parameters, CPs with different net topologies could also be derived from the same set of starting materials. These results would be reported in due course.

Thermal analysis. To understand the thermal stability of the new CPs, thermogravimetric (TG) analyses were performed (Fig. S8 in the ESI†). The TG curve of **1** with a 2D net shows the release of a coordinated water molecules at 92–185 ºC with an observed weight loss of 3.90 % (calculated = 3.97 %). Above 275 ºC, the polymeric structure disintegrates. Complex **2** featuring a **dia** net is more thermally stable. The material loses the coordinated water molecule at 60–263 ºC, with an observed mass loss of 2.00 %, which is consistent with the theoretical value of 2.11 %. Beyond 323 ºC, the decomposition of **2** occurs. Complex **3** exhibits the first weight loss of 14.29 % at 215–343 ºC, corresponding to the release of one half of L1 and OH ligand (calculated = 14.07 %). A second weight loss occurs at 401–567 ºC, corresponding to

the decomposition of the two-fold interpenetrating **pcu** framework. The TG curve of **4** exhibits an initial weight loss of 3.80 % at 149–323 ºC, corresponding to the release of the lattice and coordinated water molecules (calculated = 3.23%). Among the five CPs, **4** featuring the (3,8)-connected binodal net with tetranuclear Zn clusters as SBUs is the most thermally robust. It starts to disintegrate at a very high temperature of 466 ºC. An initial weight loss of 3.10 % at 94–159 ºC occurs in **5**, which is attributable to the release of the coordinated water molecule (calculated = 3.02 %). The **sra** or **rtl** framework in **5** then decomposes at 351 ºC. Overall, the TG analyses showed that the 3D nets in **2**–**5** are more robust than the 2D framework of **1**. Complex **3** and **4** featuring the tetranuclear Zn clusters as SBUs are more robust than **2** and **5** which consist of the dinuclear metal clusters. The higher thermal stability of **4** than **3** may be due to the more compact nature of the tetranuclear SBUs in **4** (see Fig. 3a and b).

Luminescent properties. The solid-state emission spectra for the new Zn CPs as well as free 1,4-bdcH_2 and 1,3,5-btcH_3 were investigated at room temperature (Fig. 9). The emission bands of free 1,4-bdcH_2 and 1,3,5-btcH_3 at 439 and 434 nm upon excitation at 325 and 331 nm, respectively, can be ascribed to the $\pi^* \rightarrow$ n transitions. Free L1 (λ_{max} = 401 upon excitation at 308 nm) and L2 (λ_{max} = 391 upon excitation at 318 nm) are also emissive (Fig. S9 in the ESI†). For compound **3**, the intense emission band observed at 380 nm (λ_{ex} = 330 nm) can be assigned to the intraligand transition of the L1 ligand. Interestingly, there is no fluorescent contribution from 1,4-bdc at ca. 440 nm, which might be related to the fluorescence quenching of its carboxyl groups.[26] In contrast, for compound **4**, an intense emission band was observed at 480 nm (λ_{ex} = 330 nm), which means a red shift of 46 nm with respect to the emission of the free 1,3,5-btcH_3. This intense band can be ascribed to the ligand-to-metal charge transfer (LMCT) involving the ligand-stabilized Zn_4O cluster unit.[2a, 27] For compound **5**, emission bands at 370 and 443 nm (λ_{ex} = 325

nm) can be assigned to the intraligand transitions of L1 and 1,3,5-btcH$_3$, respectively.

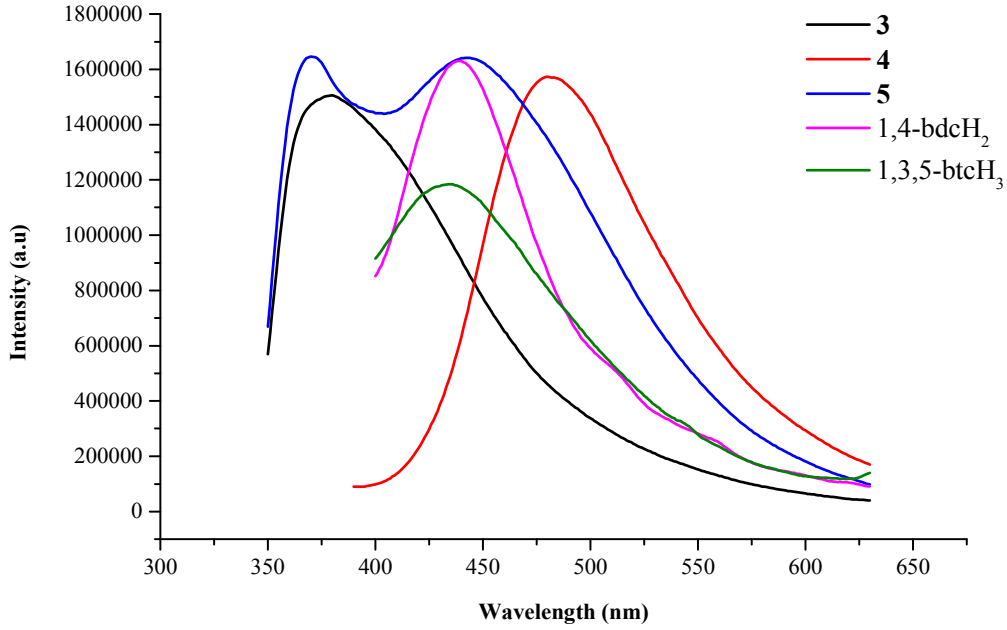

Fig. 9. Solid-state emission spectra of **3**–**5** and free ligands

Conclusion

We have successfully utilized the isomeric pair of hybrid ligands L1 and L2 containing pyridine and imidazole donors in the construction of novel 2D and 3D Ni(II) and Zn(II) CPs with a diversity of net topologies including a rare 2D 4-connected net in **1**, a **dia** net in **2**, a two-fold interpenetrating **pcu** net in **3**, a rare 3D (3,8)-connected binodal net in **4**, and **sra** and **rtl** nets in **5**. All the nets in these complexes, except that in **1**, were formed based on SBUs, accounting for their high thermal stability. In particular, the high robustness of the framework in **4** can be attributed to the presence of the compact tetranuclear $Zn_4(CO_2)_4(\mu^4\text{-}O)(\mu^2\text{-}H_2O)O_2$ SBUs. Interestingly, using the same reaction conditions of **1**–**4**, complex **5** was obtained together with another crystalline phase. Simple tuning of the heating temperature and duration allowed the isolation of **5** in pure form. By further manipulation of the reaction parameters, other CPs could

be obtained and these results would be reported in due course.

Experimental

General information. Solvents were dried with standard procedures. Starting chemicals were purchased from commercial source and used as received. The infrared spectra were acquired from a Varian Cary 640 infrared spectrophotometer. The emission spectra were measured on a Varian Cary Eclipse spectrometer. Elemental analyses were performed on a Thermo Flash 2000 CHN-O elemental analyzer. Thermogravimetric analysis (TGA) was performed on a Perkin-Elmer Pyris 6 thermogravimetric analyzer under flowing N_2 gas (20 mL/min), and the heating rate was 20 °C/min. 3-Pyridin-3-ylimidazo[1,2-a]pyridine (L1) and 3-pyridin-4-ylimidazo[1,2-a]pyridine (L2) were prepared according to the literature procedure.[14]

Synthesis of $[Ni(1,4\text{-bdc})(L1)(H_2O)_2]_n$ (1). $Ni(NO_3)_2{\cdot}6H_2O$ (0.391 g, 1.54 mmol), L1 (0.100 g, 0.512 mmol), and terephthalic acid (0.170 g, 1.02 mmol) were placed in H_2O (8 mL) and DMF (2 mL) in a 20 mL Teflon-lined stainless reactor. The reactor was tightly closed and heated up to 140 °C in 12 h and maintained at the same temperature for 48 h. Afterward, the reaction mixture was allowed to cool down to room temperature at a rate of –4 °C/h. Green crystals were obtained and they were separated by filtration, washed with deionized water, DMF, and dichloromethane, and then dried in air. Yield: 0.220 g, 95%. Anal. Calcd for $C_{20}H_{17}NiN_3O_6$: C, 52.90; H, 3.77; N, 9.25. Found: C, 52.69; H, 4.08; N, 9.23. IR (KBr/pellet, cm^{-1}): 3077.8 (w, br), 1947.7 (w), 1818.5 (w), 1747.2 (w), 1641 (w), 1602.5 (w), 1552.4 (s), 1500.3 (w), 1446.3 (w), 1419.3 (w), 1380.7 (s), 1299.7 (w), 1184.0 (m, sh), 1157.0 (m), 1087.6 (w), 1056.8 (w), 1020.1 (m), 987.3 (w), 941.0 (w), 921.8 (w), 875.5 (m), 831.1 (m), 748.2 (s, br), 709.6 (m), 636.3 (m), 553.4 (m), 507.1 (m).

Synthesis of $[Ni_2(1,3\text{-bdc})_2(L1)_2(H_2O)]_n$ (2). $Ni(NO_3)_2{\cdot}6H_2O$ (0.130 g, 0.512 mmol), L1 (0.100 g, 0.512 mmol), and isophthalic acid (0.0430 g, 0.256 mmol) were placed in H_2O (8 mL) and DMF (2 mL) in a 20 mL Teflon-lined stainless reactor. The heating and workup procedures followed those for **1**. Blue-green crystals were obtained. Yield: 0.110 g, 50%. Anal. Calcd for $C_{40}H_{28}Ni_2N_6O_9{\cdot}H_2O$: C, 55.09; H, 3.47; N, 9.64. Found: C, 54.70; H, 3.87; N, 10.08. IR (KBr/pellet, cm^{-1}): 3062.4 (w, br), 2356.6 (w), 1681.6 (m, sh), 1631.4 (m, br), 1583.2 (w), 1536.9 (w, br), 1500.3 (m), 1475.2 (w), 1438.6 (m), 1382.7 (s), 1299.7 (m), 1268.9 (w), 1180.2 (m), 1151.3 (m), 1072.2 (m, br), 1031.7 (w), 1010.5 (w), 979.6 (w), 914.0 (w, br), 808.0 (m), 740.5 (s), 711.6 (s), 657.6 (w), 634.4 (w), 551.5 (w, br).

Synthesis of $[Zn_2(1,4\text{-bdc})_{1.5}(L1)(OH)]_n$ (3). $Zn(NO_3)_2{\cdot}6H_2O$ (0.457 g, 1.54 mmol), L1 (0.100 g, 0.512 mmol), and terephthalic acid (0.170 g, 1.02 mmol) were placed in H_2O (8 mL) and DMF (2 mL) in a 20 mL Teflon-lined stainless reactor. The heating and workup procedures followed those for **1**. Pale orange-yellow crystals were obtained. Yield: 0.260 g, 88%. Anal. Calcd for $C_{24}H_{16}N_3O_7Zn_2$: C, 48.92; H, 2.74; N, 7.13. Found: C, 48.69; H, 2.83; N, 7.16. IR (KBr/pellet, cm^{-1}): 3129.9 (w), 3097.1 (w), 3052.7 (w), 1592.9 (s, br), 1529.2 (w), 1502.2 (m), 1376.9 (s), 1297.8 (w), 1195.6 (m), 1172.5 (w), 1141.6 (w), 1068.3 (w), 1020.1 (w), 985.4 (w), 925.6 (w), 885.1 (w), 863.9 (w), 835.0 (m, br), 744.4 (s, sh), 698.1 (w), 642.1 (w), 574.6 (w), 536.1 (m).

Synthesis of $[Zn_2(1,3,5\text{-btc})(L1)O_{0.5}(H_2O)_{0.5}{\cdot}H_2O]_n$ (4) $Zn(NO_3)_2{\cdot}6H_2O$ (0.152 g, 0.512 mmol), L1 (0.100 g, 0.512 mmol), and 1,3,5-benzenetricarboxylic acid (0.0540 g, 0.256 mmol) were placed in H_2O (8 mL) and DMF (2 mL) in a 20 mL Teflon-lined stainless reactor. The heating and workup procedures followed those for **1**. Yellow crystals were obtained. Yield: 0.120 g, 82%. Anal. Calcd for $C_{21}H_{15}N_3O_8Zn_2$: C, 44.36; H, 2.75; N, 7.39. Found: C, 44.36; H, 2.61; N, 7.36. IR (KBr/pellet, cm^{-1}): 3091.3 (w, br), 2356.6

(w) 1631.4 (s), 1581.3 (m, br), 1502.2 (m, sh), 1471.4 (w), 1436.7 (s), 1369.2 (s), 1301.7 (w), 1186.0 (m), 1159.0 (w), 1101.1 (w), 1058.7 (w), 1031.7 (w, br), 989.3 (w), 923.7 (m, br), 860.1 (w), 815.7 (w), 763.6 (s), 711.6 (s), 644.1 (w), 601.6 (m), 543.8 (w).

Synthesis of $[Zn_2(1,3,5\text{-btc})(L2)(OCOH)(H_2O)]_n$ (5). $Zn(NO_3)_2{\cdot}6H_2O$ (0.305 g, 1.02 mmol), L2 (0.100 g, 0.512 mmol), and 1,3,5-benzenetricarboxylic acid (0.108 g, 0.512 mmol) were placed in H_2O (8 mL) and DMF (2 mL) in a 20 mL Teflon-lined stainless reactor. The reactor was tightly closed and heated up to 150 °C in 1 h and maintained at the same temperature for 24 h. Afterward, the reaction mixture was allowed to cool down to room temperature at a rate of –37 °C/h. Orange yellow crystals were obtained and they were separated by filtration, washed with deionized water, DMF, and dichloromethane, and then dried in air. Yield: 0.230 g, 76%. Anal. Calcd for $C_{22}H_{14}N_3O_9Zn_2$: C, 44.39; H, 2.37; N, 7.06. Found: C, 44.31; H, 2.69; N, 6.92. IR (KBr/pellet, cm^{-1}): 3108.7 (w, br), 3077.8 (w, br), 3046.9 (w, br), 2352.7 (w), 1644.9 (s), 1619.9 (m), 1556.2 (m, br), 1494.5 (m), 1444.4 (m), 1373.1 (m, br), 1336.4 (m, br), 1222.6 (w), 1184.0 (w), 1164.8 (w), 1105.0 (w), 1070.3 (w), 1033.6 (w), 991.2 (w), 925.6 (w), 881.3 (w), 835.0 (w), 763.6 (m), 727.0 (s), 588.1 (w), 543.8 (m).

X-ray diffraction studies. Samples were collected at 150(2) K on a Bruker APEX II equipped with a CCD area detector and a graphite monochromater utilizing MoKα radiation (λ = 0.71073 Å). The unit cell parameters were obtained by least-squares refinement. Data collection and reduction were performed using the Bruker APEX2 and SAINT software.[28] Absorption corrections were performed using the SADABS program.[29] All the structures were solved by direct methods and refined by full-matrix least squares methods against F^2 with the SHELXTL software package.[30] All non-H atoms were refined anisotropically. All H-atoms upon carbons were fixed at calculated positions and refined with the use of a riding model. The

H-atoms upon water molecules in **1** were located from difference maps and refined with isotropic temperature factors. Electron density attributed to heavily disordered solvent in **2** was removed from the structure (and the corresponding F_o) with the SQUEEZE procedure implemented in PLATON.[17] The H1 atom in **2** was located from the difference map and refined with isotropic temperature factors. The O5–H1 distance was restrained to 0.889 Å. The H7a atom in **3** was located from the difference map and not refined. The H8 atom in **4** was located from the difference map and the O8–H8 distance was restrained to 0.810 Å. Hydrogen atoms on O9 were not located. The H7A and H7B atoms in **5** were located from the difference map and their O–H distances were restrained to 0.810 Å. The H8A and H8B atoms in **6** were located from the difference map and their O–H distances were restrained to 0.860 Å. Hydrogen atoms upon O1 were not located. Crystallographic data are listed in Table S1 of the ESI†. X-ray crystallographic information files (CIF) are available for compounds **1**–**6**. This material is available free of charge via the Internet at http://pubs.acs.org. The CIF are also available from the Cambridge Crystallographic Data Centre (CCDC) upon request (http://www.ccdc.cam.ac.uk/data_request/cif, CCDC deposition numbers CCDC 998457–998459, 998461–998462 and 1012147.

Acknowledgements. We are grateful to the Ministry of Science and Technology of Taiwan for financial support of this work. We also thank the National Center for High-performance Computing of Taiwan for computing time and financial support of the Conquest software.

†Electronic supplementary information (ESI) available: PXRD traces for **1**–**5**, TG curves for **1**–**5**, solid-state emission spectra for **3**–**5**, absorption and excitation spectra for L1, L2 and **3**–**5**, a table of crystallographic data for **1**–**6**, a table of hydrogen bonds for **2**, and structural data and drawings for **6**. CCDC 998457–998459, 998461–998462 and 1012147.

Table 1. Important bond distances (Å) and angles (°) of **1** and **2**.

1		**2**	
Ni1–N1	2.097(4)	Ni1–N1#4	2.087(3)
Ni1–N3	2.062(4)	Ni1–N2	2.116(3)
Ni1–O1	2.044(3)	Ni1–O1	2.055(2)
Ni1–O3	2.113(4)	Ni1–O2#2	2.015(2)
Ni1–O4	2.092(4)	Ni1–O4#3	2.096(2)
Ni1–O6#1	2.036(4)	Ni1–O5	2.0348(16)
N1–Ni1–O3	178.58(16)	N1#4–Ni1–N2	92.02(10)
N3–Ni1–N1	87.85(16)	O1–Ni1–N1#4	89.92(9)
N3–Ni1–O3	93.45(16)	O1–Ni1–N2	94.19(10)
N3–Ni1–O4	177.99(16)	O1–Ni1–O4#3	176.79(9)
O1–Ni1–N1	91.45(15)	O2#2–Ni1–N1#4	87.62(10)
O1–Ni1–N3	94.32(14)	O2#2–Ni1–N2	176.23(11)
O1–Ni1–O3	89.02(14)	O2#2–Ni1–O1	89.56(10)
O1–Ni1–O4	84.48(14)	O2#2–Ni1–O4#3	88.04(10)
O4–Ni1–N1	93.78(16)	O2#2–Ni1–O5	91.00(8)
O4–Ni1–O3	84.92(13)	O4#3–Ni1–N1#4	87.86(9)
O6#1–Ni1–N1	94.12(15)	O4#3–Ni1–N2	88.20(10)
O6#1–Ni1–N3	90.54(15)	O5–Ni1–N1#4	177.38(8)
O6#1–Ni1–O1	172.74(14)	O5–Ni1–N2	89.21(9)
O6#1–Ni1–O3	85.31(14)	O5–Ni1–O1	92.29(9)
O6#1–Ni1–O4	90.51(15)	O5–Ni1–O4#3	89.87(8)

Symmetry code for **1**: #1 = x + 1/2, y, z – 1/2. **2**: #1 = x + 1/4, –y + 1/4, z + 1/4; #2 = –x + 2, –y, z; #3 = –x + 7/4, y – 1/4, z + 1/4; #4 = x – 1/4, –y + 1/4, z – 1/4

Table 2. Important bond distances (Å) and angles (°) of **3**.

Zn1–C13	2.502(4)	Zn2–O7#1	1.949(2)
Zn1–N1	2.102(3)	Zn2–O4#2	1.965(3)
Zn1–O7#1	2.040(2)	Zn2–N2#3	1.995(3)
Zn1–O1	2.146(3)	Zn2–O6	1.968(2)
Zn1–O2	2.217(2)		
Zn1–O5	2.118(2)		
N1–Zn1–C13	122.12(12)	O7#1–Zn1–N1	102.35(10)
N1–Zn1–O1	91.87(10)	O7#1–Zn1–O1	162.87(9)
N1–Zn1–O2	151.68(11)	O7#1–Zn1–O2	105.94(9)
N1–Zn1–O5	87.55(10)	O7#1–Zn1–O5	93.62(9)

N1–Zn1–O7	103.78(10)	O7#1–Zn1–O7	79.26(10)
O1–Zn1–C13	30.34(10)	O7–Zn1–C13	83.67(10)
O1–Zn1–O2	60.48(9)	O7–Zn1–O2	82.74(9)
O1–Zn1–O7	88.18(9)		
O2–Zn1–C13	30.17(10)	O4#2–Zn2–N2#3	100.01(11)
O5–Zn1–C13	94.59(11)	O4#2–Zn2–O3	109.80(11)
O5–Zn1–O1	96.52(10)	O6–Zn2–N2#3	105.46(11)
O5–Zn1–O2	89.60(10)	O7#1–Zn2–N2#3	115.35(10)
O5–Zn1–O7	167.62(9)	O7#1–Zn2–O4#2	116.94(10)
O7#1–Zn1–C13	135.02(10)	O7#1–Zn2–O6	108.53(10)

Symmetry code: #1 = –x + 2, –y + 2, –z + 1; #2 = x + 1, y, z + 1; #3 = x, y + 1, z + 1

Table 3. Important bond distances (Å) and angles (°) of **4**.

Zn1–N1	2.185(5)	Zn2–N2	1.996(5)
Zn1–O1	2.123(4)	Zn2–O2	2.028(4)
Zn1–O3	2.134(4)	Zn2–O4	1.980(4)
Zn1–O5	2.038(3)	Zn2–O5	1.909(3)
Zn1–O6	2.059(4)		
Zn1–O8	2.251(6)		
Zn1–Zn2	3.0130(10)		
O5–Zn1–O6	94.30(13)	O6–Zn1–Zn2	122.56(12)
O5–Zn1–O1	98.03(18)	O1–Zn1–Zn2	76.55(12)
O6–Zn1–O1	83.31(17)	O3–Zn1–Zn2	67.84(12)
O5–Zn1–O3	100.04(13)	N1–Zn1–Zn2	147.07(13)
O6–Zn1–O3	164.39(19)	O8–Zn1–Zn2	98.29(13)
O1–Zn1–O3	88.57(19)		
O5–Zn1–N1	171.38(18)	O5–Zn2–O4	118.8(2)
O6–Zn1–N1	84.79(18)	O5–Zn2–N2	126.39(19)
O1–Zn1–N1	90.39(19)	O4–Zn2–N2	101.3(2)
O3–Zn1–N1	81.94(18)	O5–Zn2–O2	107.54(13)
O5–Zn1–O8	79.1(2)	O4–Zn2–O2	95.97(19)
O6–Zn1–O8	101.92(13)	N2–Zn2–O2	100.3(2)
O1–Zn1–O8	174.17(14)	O5–Zn2–Zn1	41.86(9)
O3–Zn1–O8	86.93(15)	O4–Zn2–Zn1	90.37(13)
N1–Zn1–O8	92.6(2)	N2–Zn2–Zn1	166.88(16)
O5–Zn1–Zn2	38.68(6)	O2–Zn2–Zn1	81.57(13)

Table 4. Important bond distances (Å) and angles (°) of **5**.

Zn1–N1	2.013(4)	Zn2–N3#5	2.027(5)
Zn1–O1	1.961(4)	Zn2–O5	1.987(4)
Zn1–O3#4	1.920(4)	Zn2–O6	2.463(4)
Zn1–O2#2	2.021(4)	Zn2–O7	1.874(4)
		Zn2–O8	1.944(5)
O3#4–Zn1–O1	121.67(16)	O8–Zn2–O5	109.75(18)
O3#4–Zn1–N1	106.09(19)	O7–Zn2–N3#5	105.1(2)
O1–Zn1–N1	114.28(17)	O8–Zn2–N3#5	96.6(2)
O3#4–Zn1–O2#2	111.20(16)	O5–Zn2–N3#5	126.57(19)
O1–Zn1–O2#2	100.58(15)	O7–Zn2–O6	92. 23(13)
N1–Zn1–O2#2	101.05(17)	O8–Zn2–O6	165.09(18)
		O5–Zn2–O6	58.08(16)
O7–Zn2–O8	101.20(17)	N3#5–Zn2–O6	85.98(17)
O7–Zn2–O5	113.68(18)		

Symmetry code: #1 = –x + 1, y + 1/2, –z + 1/2; #2 = –x + 1, –y + 2, –z + 1; #3 = x – 1, y, z – 1; #4 = x + 1, y, z + 1; #5 = –x + 1, y – 1/2, –z + 1/2

Notes and references

1 (a) A. U. Czaja, N. Trukhan and U. Muller, *Chem. Soc. Rev.*, 2009, **38**, 1284; (b) G. Ferey, *Chem. Soc. Rev.*, 2008, **37**, 191; (c) C. Janiak, *Dalton Trans.*, 2003, 2781; (d) C. Wang, D. Liu and W. Lin, *J. Am. Chem. Soc.*, 2013, **135**, 13222.

2 (a) M. D. Allendorf, C. A. Bauer, R. K. Bhakta and R. J. T. Houk, *Chem. Soc. Rev.*, 2009, **38**, 1330; (b) Y. Cui, Y. Yue, G. Qian and B. Chen, *Chem. Rev.*, 2011, **112**, 1126; (c) J. Heine and K. Muller-Buschbaum, *Chem. Soc. Rev.*, 2013, **42**, 9232.

3 M. Kurmoo, *Chem. Soc. Rev.*, 2009, **38**, 1353.

4 A. Nalaparaju and J. Jiang, *J. Phy. Chem. C*, 2012, **116**, 6925.

5 P. Horcajada, R. Gref, T. Baati, P. K. Allan, G. Maurin, P. Couvreur, G. Férey, R. E. Morris and C. Serre, *Chem. Rev.*, 2011, **112**, 1232.

6 M. Yoon, R. Srirambalaji and K. Kim, *Chem. Rev.*, 2011, **112**, 1196.

7 (a) J. L. C. Rowsell and O. M. Yaghi, *Microporous and Mesoporous Mater.*, 2004, **73**, 3; (b) L. J. Murray, M. Dinca and J. R. Long, *Chem. Soc. Rev.*, 2009, **38**, 1294; (c) J. L. C.Rowsell and O. M. Yaghi, *Angew. Chem. Int. Ed.*, 2005, **44**, 4670.

8 L. E. Kreno, K. Leong, O. K. Farha, M. Allendorf, R. P. Van Duyne and J. T. Hupp, *Chem. Rev.*, 2011, **112**, 1105.

9 J.-R. Li, J. Sculley and H.-C. Zhou, *Chem. Rev.*, 2011, **112**, 869.

10 (a) O. K. Farha and J. T. Hupp, *Acc. Chem. Res.*, 2010, **43**, 1166; (b) H.-L. Jiang, T. A. Makal and H.-C. Zhou, *Coord. Chem. Rev.*, 2013, **257**, 2232; (c) F. A. Almeida Paz, J. Klinowski, S. M. F. Vilela, J. P. C. Tome, J. A. S. Cavaleiro and J. Rocha, *Chem. Soc. Rev.*, 2012, **41**, 1088.

11 (a) B.-Q. Ma, K. L. Mulfort and J. T. Hupp, *Inorg. Chem.*, 2005, **44**, 4912; (b) B. Chen, C. Liang, J. Yang, D. S. Contreras, Y. L. Clancy, E. B. Lobkovsky, O. M. Yaghi and S. Dai, *Angew. Chem. Int. Ed.*, 2006, **45**, 1390; (c) S.-H. Cho, B. Ma, S. T. Nguyen, J. T. Hupp and T. E. Albrecht-Schmitt, *Chem. Commun.*, 2006, 2563; (d) H. Chun, D. N. Dybtsev, H. Kim and K. Kim, *Chem. Eur. J.*, 2005, **11**, 3521.

12 (a) J. Yang, J.-F. Ma, Y.-Y. Liu and S. R. Batten, *CrystEngComm*, 2009, **11**, 151; (b) Y.-Y. Liu, Z.-H. Wang, J. Yang, B. Liu, Y.-Y. Liu and J.-F. Ma, *CrystEngComm*, 2011, **13**, 3811; (c) Y. Qi, F. Luo, Y. Che and J. Zheng, *Cryst. Growth Des.*, 2007, **8**, 606; (d) L.-P. Zhang, J.-F. Ma, Y.-Y. Pang, J.-C. Ma and J. Yang, *CrystEngComm*, 2010, **12**, 4433; (e) P.-K. Chen, Y. Qi, Y.-X. Che and J.-M. Zheng, *CrystEngComm*, 2010, **12**, 720; (f) J.-Y. Lee, C.-Y. Chen, H. M. Lee, E. Passaglia, F. Vizza and W. Oberhauser, *Cryst. Growth Des.*, 2011, **11**, 1230; (g) C.-H. Ke, G.-R. Lin, B.-C. Kuo and H. M. Lee, *Cryst. Growth Des.*, 2012, **12**, 3758; (h) H.-J. Lee, P.-Y. Cheng, C.-Y. Chen, J.-S. Shen,

D. Nandi and H. M. Lee, *CrystEngComm*, 2011, **13**, 4814.

13 (a) C.-S. Liu, P.-Q. Chen, E.-C. Yang, J.-L. Tian, X.-H. Bu, Z.-M. Li, H.-W. Sun and Z. Lin, *Inorg. Chem.*, 2006, **45**, 5812; (b) J. Xu, X. Sun, X. Yan, S. Wang and M. Sun, *Inorg. Chem. Commun.*, 2013, **37**, 49.

14 H. Y. Fu, L. Chen and H. Doucet, *J. Org. Chem.*, 2012, **77**, 4473.

15 V. A. Blatov, A. P. Shevchenko and V. N. Serezhkin, *J. Appl. Crystallogr.*, 2000, **33**, 1193.

16 V. A. Blatov, M. O'Keeffe and D. M. Proserpio, *CrystEngComm*, 2010, **12**, 44.

17 A. L. Spek, *Acta Crystallogr.*, 2009, D**65**, 148.

18 M. Eddaoudi, D. B. Moler, H. Li, B. Chen, T. M. Reineke, M. O'Keeffe and O. M. Yaghi, *Acc. Chem. Res.*, 2001, **34**, 319.

19 E. V. Alexandrov, V. A. Blatov, A. V. Kochetkov and D. M. Proserpio, *CrystEngComm*, 2011, **13**, 3947.

20 (a) C. Zhang, M. Zhang, L. Qin and H. Zheng, *Cryst. Growth Des.*, 2013, **14**, 491; (b) D. Liu, Z.-G. Ren, H.-X. Li, Y. Chen, J. Wang, Y. Zhang and J.-P. Lang, *CrystEngComm*, 2010, **12**, 1912.

21 X.-J. Li, F.-L. Jiang, M.-Y. Wu, L. Chen, J.-J. Qian, K. Zhou, D.-Q. Yuan and M.-C. Hong, *Inorg. Chem.*, 2013, **53**, 1032.

22 (a) H. K. Chae, M. Eddaoudi, J. Kim, S. I. Hauck, J. F. Hartwig, M. O'Keeffe and O. M. Yaghi, *J. Am. Chem. Soc.*, 2001, **123**, 11482; (b) Q. Yue, Q. Sun, A.-L. Cheng and E.-Q. Gao, *Cryst. Growth Des.*, 2009, **10**, 44.

23 (a) R. S. Crees, M. L. Cole, L. R. Hanton and C. J. Sumby, *Inorg. Chem.*, 2010, **49**, 1712; (b) R. Singh, M. Ahmad and P. K. Bharadwaj, *Cryst. Growth Des.*, 2012, **12**, 5025.

24 (a) L.-N. Jia, L. Hou, L. Wei, X.-J. Jing, B. Liu, Y.-Y. Wang and Q.-Z. Shi, *Cryst. Growth Des.*, 2013, **13**, 1570; (b) S.-C. Chen, Z.-H. Zhang, Q. Chen, H.-B. Gao, Q. Liu, M.-Y. He and M. Du, *Inorg. Chem. Commun.*, 2009, **12**, 835; (c) X. Liu, X. Wang, T. Gao, Y. Xu, X. Shen and D. Zhu, *CrystEngComm*, 2014, **16**, 2779; (d) R. Luo, H. Xu, H.-X. Gu, X. Wang, Y. Xu, X. Shen, W. Bao and D.-R. Zhu, *CrystEngComm*, 2014, **16**, 784.

25 (a) F. Dai, D. Sun and D. Sun, *Cryst. Growth Des.*, 2011, **11**, 5670; (b)J. F. Eubank, L.Wojtas, M. R. Hight, T. Bousquet, V. C. Kravtsov and M. Eddaoudi, *J. Am. Chem. Soc.*, 2011, **133**, 17532.

26 N. Wang, J.-G. Ma, W. Shi and P. Cheng, *CrystEngComm*, 2012, **14**, 5198.

27 Y. Ma, T. Lai and Y. Wu, *Adv. Mater.*, 2000, **12**, 433.

28 Bruker AXS Inc., Madison, Wisconsin, USA., 2007.

29 G. M. Sheldrick, University of Göttingen, Germany, 1996.

30 G. Sheldrick, *Acta Crystallogr.*, 2008, **A64**, 112.

Table of contents entry

Tuning of net architectures of Ni(II) and Zn(II) coordination polymers using isomeric organic linkers

*Shuang-De Liu, Bing-Chiuan Kuo, Yen-Wen Liu, Jing-Yi Lee, Kwun Yip Wong and Hon Man Lee**

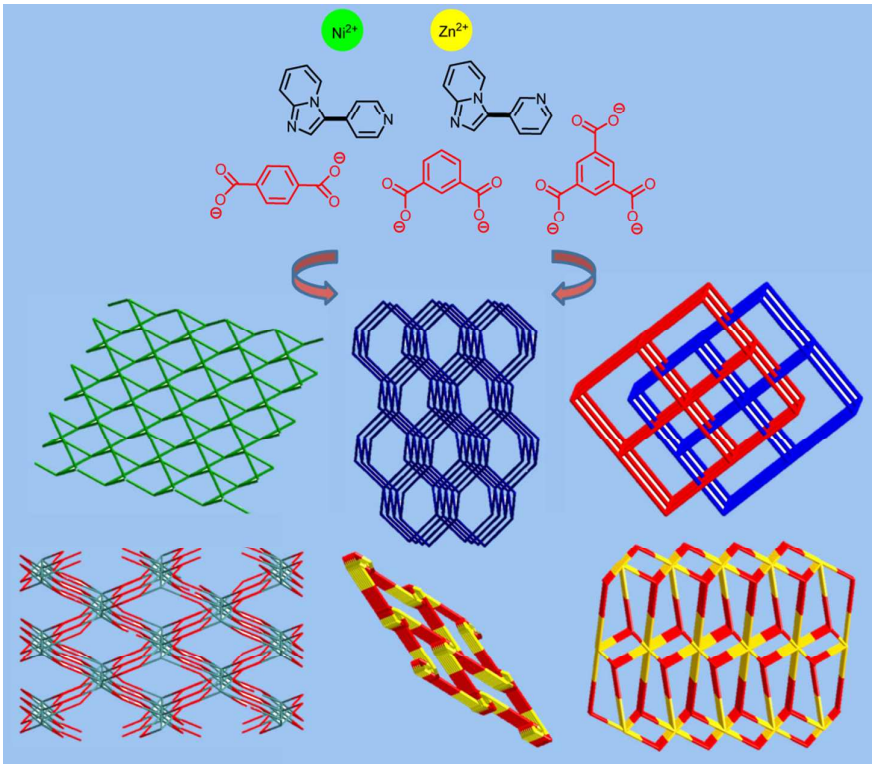

Synopsis

Ni(II) and Zn(II) coordination polymers with diverse net topologies were synthesized using isomeric organic linkers.